

See discussions, stats, and author profiles for this publication at: <https://www.researchgate.net/publication/331452811>

# Investigating the effects of numerical discretization and turbulence modeling on the accuracy of flow solution around NACA0012 airfoil using OpenFOAM

Conference Paper · March 2012

CITATIONS

0

READS

28

1 author:



**Ehsan Roohi**

Ferdowsi University Of Mashhad

117 PUBLICATIONS 1,305 CITATIONS

SEE PROFILE

Some of the authors of this publication are also working on these related projects:



shale gas [View project](#)



DSMC collision scheme improvement [View project](#)



# Investigating the effects of numerical discretization and turbulence modeling on the accuracy of flow solution around NACA0012 airfoil using OpenFOAM

FarshadRezaei,Ehsan Roohi, MahmoodPasandideh-Fard

Department of Mechanical Engineering, Ferdowsi University of Mashhad  
Mashhad, Iran, P.O.Box: 91775-1111  
e.roohi@um.ac.ir

## Abstract

In this paper, we study the influence of grid size, finite volume discretization schemes, Reynolds number, and turbulence modeling on the accuracy of numerical solution over NACA0012 airfoil using the OpenFOAM package. Different grid sizes have been examined and the suitable mesh with accurate  $C_L$  had been presented. Additionally, it was observed that the accuracy of solution increases and the error of computing  $C_L$  and  $C_D$  decreases if we suitably improve the discretization schemes of the momentum equation. Among different discretization schemes, the best result is obtained once we tried linear discretization method for the convective term and fourth order discretization method for the pressure gradient term. The effect of Reynolds number on the accuracy of solution has also been investigated and it was found that  $C_L$  and  $C_D$  becomes more accurate at higher Reynolds numbers. Additionally, we tried two turbulence models, i.e., Spalart-Allmaras and K- $\omega$  SST and compared drag coefficient of two models.

**Keywords:** *NACA 0012 airfoil, finite volume method, OpenFOAM, discretisation scheme, turbulence models.*

## Introduction

Incompressible flow around NACA 0012 airfoil had been the subject of many studies during the last decades. Ladson [1] investigated Mach and Reynolds number effects on the aerodynamic behavior of the NACA0012 airfoil. His results showed that changes in Mach number affected lift-curve slope and maximum lift coefficient. Moreau et al. [2] performed LES (Large Eddy Simulation) of the trailing edge flow and noise of a NACA0012 airfoil near stall condition. IM et al. [3] performed DES (Detached Eddy Simulation) and DDES (Delayed Detached Eddy Simulation) of NACA0012 airfoil near stall condition. They showed that DDES and DES predicted the drag coefficient accurately, while URANS (unsteady Reynolds-averaged Navier-Stokes) overpredicted the drag by 33.6%.

Different researchers employed OpenFOAM for aerodynamic proposes. For example, Verhoeven [4] investigated trailing edge noise simulation using IDDES (Improved Delayed Detached Eddy Simulation). He used different meshes. However, he reported that the response of the IDDES turbulence model to different employed meshesis unclear and requires further investigation. Abedi [5] investigated OpenFOAM solution for incompressible flow around a 2D-airfoil in

order to compute the lift and drag coefficients during transition from laminar to turbulent flow.

As the above mentioned literature survey shows, there is not detailed investigation and validation of flow field around NACA0012 airfoil using OpenFOAM package. Accurate numerical simulation of flow field over external geometries needs considering different points such as employing suitable grid size (especially in the boundary layer), applying accurate discretization schemes (specifically for momentum equation), and consideration of suitable turbulence model. In this paper, we have numerically examined incompressible flow around NACA 0012 using the open source CFD toolbox of OpenFOAM. Within the framework of OpenFOAM, we used simpleFoam solver for analyzing NACA 0012 airfoil[5]. SIMPLE algorithm was used for pressure-velocity coupling. We performed our simulation using different grid size in the boundary layer, different discretization schemes for the momentum equation, different Reynolds numbers and two turbulence models. Conclusions on using best combination of the considered parameters have been suggested.

## Computational methodology

The numerical simulation reported in the present work have been conducted using OpenFOAM 2.1.0 code. OpenFoam has attracted much attention recently because it is a sustainable open source code designed for a wide range of CFD applications. It is a C++ toolbox based on a object oriented programming [6]. OpenFOAM is released under the GPL [7-8] and it consists of enormous groups of libraries for different mathematical, numerical and physical models. Linking the mathematical/numerical tools with the physical models in a main C++ function produces different solvers and utilities. The simulations reported here in were conducted using the simpleFoam solver of OpenFOAM. This solver is a steady-state solver for incompressible turbulent flow. OpenFOAM allows the users freely choose among a wide range of numerical discretization and interpolation schemes.

## The simpleFoam solver

SimpleFoam is a pressure-based solver which solves the momentum equation with under relaxation factors and then iteratively applies a pressure correctors equation based on the conservation of mass to evaluate the velocity and pressure fields. The turbulence model equations are solved after the velocity and pressure are computed at each time step, and an iterative update is

performed on the later fields before a consecutive step is performed.

### The SIMPLE algorithm

The Semi-Implicit Method of Linked Equations (SIMPLE) [9] is the algorithm by which the governing equations are solved in SimpleFoam solver. This algorithm solves the momentum matrix and then applies a pressure correction to conserve the incompressibility constraint implied by the continuity equation. This process is iterative. Within the main iteration conducted by the SIMPLE algorithm there is a momentum corrector step conducted to ensure that the velocity field is updated according to the new pressure values. In the present work, such momentum corrector step was conducted twice for each iteration in all cases. This was necessary to reach the convergence criterion for the pressure field.

### Turbulence Models Equations

#### Spalart-Allmaras model

Spalart-Allmaras model is an one equation model which solves a transport equation for a viscosity-like variable  $\hat{\nu}$ . This term is referred to as Spalart-Allmaras variable. The following equations represents the implementation of the Spalart-Allmaras model [10]. The one-equation model is given by:

$$\frac{\partial \hat{\nu}}{\partial t} + \mu_j \frac{\partial \hat{\nu}}{\partial x_j} = c_{b1}(1 - f_{t2})\hat{S}\hat{\nu} - \left[ c_{w1}f_w - \frac{c_{b1}}{k^2}f_{t2} \right] \left( \frac{\hat{\nu}}{d} \right)^2 + \left[ \frac{\partial}{\partial x_j} \left( (\vartheta + \hat{\nu}) \frac{\partial \hat{\nu}}{\partial x_j} \right) + c_{b2} \frac{\partial \hat{\nu}}{\partial x_i} \frac{\partial \hat{\nu}}{\partial x_i} \right] \quad (1)$$

And the turbulent eddy viscosity is computed from:

$$\mu_t = \rho \hat{\nu} f_{v1} \quad (2)$$

Where

$$f_{v1} = \frac{x^3}{x^3 + c_{v1}^3} \quad (3)$$

$$x = \frac{\hat{\nu}}{v} \quad (4)$$

$\rho$  is the density,  $v = \mu/\rho$  is the kinematic viscosity, and  $\mu$  is the molecular dynamic viscosity. Additional definitions are given by the following equations:

$$\hat{S} = \Omega + \frac{\hat{\nu}}{k^2 d^2} f_{v2} \quad (5)$$

where  $\Omega = \sqrt{2W_{ij}W_{ij}}$  is the magnitude of the vorticity,  $d$  is the distance from field point to the nearest wall, and

$$f_{v2} = 1 - \frac{x}{x f_{v1}} f_w = g \left[ \frac{1 + c_{w3}^6}{g^6 + c_{w3}^6} \right]^{1/6} \quad (6) g = r + c_{w2}(r^6 - r) \quad (7)$$

$$r = \min \left[ \frac{\hat{\nu}}{S k^2 d^2}, 10 \right] \quad (8) f_{t2} = c_{t3} \exp(-c_{t4} x^2)$$

$$(9) W_{ij} = \frac{1}{2} \left( \frac{\partial u_i}{\partial x_j} - \frac{\partial u_j}{\partial x_i} \right) \quad (10)$$

The boundary conditions are:

$$\hat{\nu}, wall = 0 \quad \hat{\nu}, far field = 3v_\infty : to : 5v_\infty \quad (11)$$

The constants are:

$$c_{b1} = 0.1355 \quad \sigma = 2/3 \quad c_{b2} = 0.622 \quad \kappa = 0.41 \quad c_{w2} = 0.3 \quad c_{w3} = 2 \quad c_{v1} = 7.1 \quad c_{t3} = 1.2 \quad (12)$$

$$c_{t4} = 0.5 \quad c_{w1} = \frac{c_{b1}}{k^2} + \frac{1 + c_{b2}}{\sigma}$$

#### k- $\omega$ SST

The k- $\omega$ SST turbulence model turbulence model is a two-equation eddy-viscosity model. The shear stress transport (SST) formulation combines the best of two worlds, i.e., k- $\epsilon$  and k- $\omega$ . The use of a k- $\omega$  formulation in the inner parts of the boundary layer makes the model directly usable all the way down to the wall through the viscous sub-layer, hence the k- $\omega$  SST model can be used as a Low-Reynolds turbulence model without any extra damping functions. The SST formulation also switches to a k- $\epsilon$  behavior in the free-stream and thereby avoids the common k- $\omega$  problem that the model is too sensitive to the inlet free-stream turbulence properties. Authors who use the k- $\omega$  SST model often merit it for its good behavior in adverse pressure gradients and separating flow. The k- $\omega$  SST model does produce a bit too large turbulence levels in regions with large normal strain, like stagnation regions and regions with strong acceleration. This tendency is much less pronounced than with a normal k- $\epsilon$  model though [11]. The following equation are used in k- $\omega$ SST formulation:

$$P - \beta^* \rho \omega k + \frac{\partial}{\partial x_j} \left[ (\mu + \sigma_k \mu_t) \frac{\partial k}{\partial x_j} \right] = \frac{\partial(\rho k)}{\partial t} + \frac{\partial(\rho u_j k)}{\partial x_j} \quad (13)$$

$$P - \beta^* \rho \omega k + \frac{\partial}{\partial x_j} \left[ (\mu + \sigma_k \mu_t) \frac{\partial k}{\partial x_j} \right] = \frac{\partial(\rho \omega)}{\partial t} + \frac{\partial(\rho u_j \omega)}{\partial x_j} = \frac{\gamma}{v_t} P - \beta \rho \omega^2 + \frac{\partial}{\partial x_j} \left[ (\mu + \sigma_{\omega k} \mu_t) \frac{\partial \omega}{\partial x_j} \right] + 2(1 - F_1) \frac{\rho \sigma_{\omega 2}}{\omega} \frac{\partial k}{\partial x_j} \frac{\partial \omega}{\partial x_j} \quad (14) P =$$

$$\tau_{ij} \frac{\partial u_i}{\partial x_j} \tau_{ij} = \mu_t \left( 2S_{ij} - \frac{2}{3} \frac{\partial u_k}{\partial x_j} \delta_{ij} \right) - \frac{2}{3} \rho k \delta_{ij} \quad (15)$$

$$S_{ij} = \frac{1}{2} \left( \frac{\partial u_i}{\partial x_j} + \frac{\partial u_j}{\partial x_i} \right) \quad (16)$$

And the turbulent eddy viscosity is computed from:

$$\mu_t = \frac{\rho a_1 k}{\max(a_1 \omega, \Omega F_2)} \quad (17)$$

Each of the constants is a blend of an inner (1) and outer (2) constant, blended via:

$$\phi = F_1 \phi_1 + (1 - F_1) \phi_2 \quad (18)$$

Where  $\phi_1$  represents constant 1 and  $\phi_2$  represents constant 2. Additional functions are given by:

$$F_1 = \tanh(\arg g_1^4) \quad (19)$$

$$\arg g_1 = \min \left[ \max \left( \frac{\sqrt{k}}{\beta^* \omega d}, \frac{500v}{d^2 \omega} \right), \frac{4\rho \sigma_{\omega 2} k}{CD_{k\omega} d^2} \right] \quad (20)$$

$$CD_{k\omega} = \max \left( 2\rho \sigma_{\omega 2} \frac{1}{\omega} \frac{\partial k}{\partial x_j} \frac{\partial \omega}{\partial x_j}, 10^{-20} \right) \quad (21)$$

$$F_2 = \tanh(\arg g_2^2) \quad (22)$$

$$\arg g_2 = \max \left( 2 \frac{\sqrt{k}}{\beta^* \omega d}, \frac{500v}{d^2 \omega} \right) \quad (23)$$

$\nu_t = \mu_t/\rho$  is the turbulent kinematic viscosity,  $d$  is the distance from the field point to the nearest wall, and  $\Omega$  is the vorticity magnitude. It is generally recommended to use a production limiter. In this reference, the term  $P$  in the  $k$ -equation is replaced by:

$$\min(P, 20\beta^* \rho \omega k) \quad (24)$$

The boundary conditions recommended are as follows:

$$\frac{U_\infty}{L} < \omega_{far\ field} < 10 \frac{U_\infty}{L} \quad (25)$$

$$\frac{10^{-5} U_\infty^2}{Re_L} < k_{far\ field} < \frac{0.1 U_\infty^2}{Re_L} \quad (26)$$

$$\omega_{wall} = 10 \frac{6\nu}{\beta_1 (\Delta d)^2} \quad (27)$$

$$k_{wall} = 0 \quad (28)$$

where " $L$  is the approximate length of the computational domain," and the combination of the two farfield values should yield a freestream turbulent viscosity between  $10^{-5}$  and  $10^{-2}$  times freestream laminar viscosity. Thus, the farfield turbulence boundary conditions are somewhat open to interpretation. Note that the turbulence variables decay (sometimes dramatically) from their set values in the farfield for external aerodynamic problems.

The constants are:

$$\gamma_1 = \frac{\beta_1}{\beta^*} - \frac{\sigma_{w1} \kappa^2}{\sqrt{\beta^*}} \gamma_2 = \frac{\beta_2}{\beta^*} - \frac{\sigma_{w2} \kappa^2}{\sqrt{\beta^*}} \quad (29)$$

$$\begin{aligned} \sigma_{k1} &= 0.85 & \sigma_{w1} &= 0.5 & \beta_1 &= 0.075 \\ \sigma_{k2} &= 1.0 & \sigma_{w2} &= 0.856 & \beta_2 &= 0.082 \\ \beta^* &= 0.09 & \kappa &= 0.41 & a_1 &= 0.31 \end{aligned} \quad (30)$$

## Results and Discussion

### Grid Independency

The computational domain and applied boundary condition is shown in Fig. 1. We considered the flow field around NACA0012 airfoil at velocity of  $80 \text{ m/s}$ . The chord length of the airfoil is  $1 \text{ m}$  and the employed turbulence models are Spalart-Allmaras and  $k-\omega$  SST. Three meshes with different cell sizes had been produced and the best of them is chosen. Table 1 presents the data of employed meshes. Among them, the mesh with 738 points around the airfoil and  $0.6 \text{ mm}$  thickness of the first boundary layer cell gives the most accurate solution.

**Table 1 –Lift coefficient for different meshes (angle of attack  $10^\circ$ )**

Mesh Name	Number of mesh points around airfoil	Thickness of first B.L cell (mm)	$C_L$	Error%
Mesh-1	450	0.6	1.0834	1.204
Mesh-2	592	0.6	1.0897	0.631
Mesh-3	738	0.6	1.0916	0.458

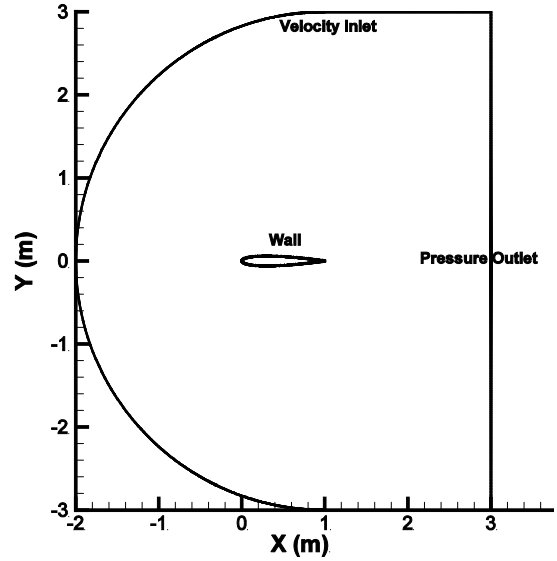


**Fig.1 Computational domain and applied boundary condition around NACA 0012airfoil**

### Investigation of Discretization Schemes of the Momentum Equation

Discretization of convective part and pressure gradient of momentum equation have proven to be one of the most troublesome parts of the computational fluid dynamics. The objective is to devise a practice that will produce a bounded, accurate and convergent solution. In this work, we are concentrated on pressure gradient, convective term and velocity interpolation of momentum equation. The momentum equation is given by:

$$\frac{\partial(\rho U)}{\partial t} + \nabla \cdot [U(\rho U)] + \nabla p + \nabla \cdot T = 0 \quad (31)$$

where  $T$  is the viscous stress tensor:

$$T = -2(\mu_{lam} + \mu_{turb}) \text{div}(D) \quad (32)$$

$D$  is deformation gradient tensor:

$$D \equiv \frac{1}{2} [\nabla u + (\nabla u)^T] \quad (33)$$

Since we consider steady state flow, discretization of time derivative term has not any influence on the accuracy of  $C_L$  and  $C_D$ .

### Pressure Gradient

At the first step, we consider the effect of discretization scheme for the pressure gradient term in the momentum equation. It was observed that by changing the pressure gradient discretization scheme from the default *Gauss linear* scheme, which is second order accurate and uses Gaussian integration, to *leastSquares*, which is second order accurate and uses least-squares integration approach, accuracy of  $C_L$  computed at  $AOA=10^\circ$  increased by %2.01 compared to thin airfoil theory. By changing the pressure gradient discretization from *Gauss linear* scheme to *fourth* scheme, which is fourth order accurate and uses least squares integration, accuracy of numerically calculated  $C_L$  has increased by %2.1 again.

### Convective Term

Next, we consider discretization of the convective term of the momentum equation, i.e.,  $(\nabla \cdot (\rho U U))$ . For an incompressible flow, we have:

$$\nabla \cdot \rho U U = \rho \left( \frac{\partial u u}{\partial x} + \frac{\partial v v}{\partial y} + \frac{\partial \omega \omega}{\partial z} \right) \quad (34)$$

We have examined the behavior of interpolation schemes used in divergence schemes and all of the cases have compared by the base case *linear-Upwind* suggested in OpenFOAM package. *QUICK*, *linear* and *SFCD* schemes have used for both  $\text{div}(\rho U, U)$  and  $\text{div}(\rho U, v)$  and the most accurate result was obtained by using *linear* scheme for  $\text{div}(\rho U, U)$ . For this case,  $C_L$  magnitude has improved by %0.35.

### Interpolation of velocity from the cell center to cell's face

In OpenFOAM, the interpolation schemes sub-dictionary contains terms that interpolate values typically from cell centers to face centers [7]. Using Spalart-Allmaras turbulence model, we have examined all of the interpolation schemes such as *linear*, *cubic-Correction*, *midpoint*, *linear-Upwind*, etc. for velocity interpolation and the results for  $C_L$  and  $C_D$  were exactly the same. There are improved versions of some of the discretization schemes for vector fields in which the limiter is formulated to take into account the direction of the flow field. These schemes are selected by adding *V* to the name of the base schemes. We also examined these improved schemes (such as *limited-Linear-V*, *vanLeer-V*, *Gamma-V*, *limited-Cubic-V* and *SFCDV*) and again  $C_L$  and  $C_D$  were not changed compared to the original schemes.

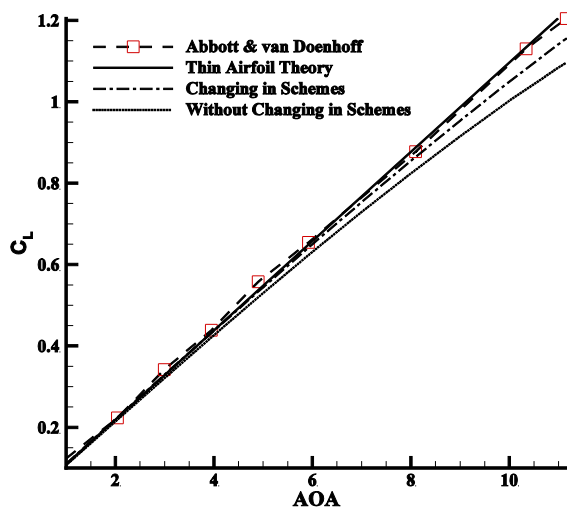


Fig. 2  $C_L$  variations vs. angle of attack from the current numerical work compared with the numerical data of Refs. [12,13] and thin airfoil theory [12]

According to the results obtained from changing the discretization schemes, the most accurate results were obtained using *fourth order* discretization scheme for pressure gradient term and *linear* scheme for divergence term  $(\rho U, U)$ . Therefore, the error in computing  $C_L$  and  $C_D$  has suitably decreased. The  $C_L$  was 0.4374 for an angle of attack  $4^\circ$ , while its value from "Thin Airfoil Theory" is 0.4386. Without two last changes in

schemes,  $C_L$  was 0.4267. The results for changing in schemes and without them are shown in Fig. 2 and are compared with Thin Airfoil Theory and Abbott & van Doenhoff data [12]. It is clear that by changing in schemes, the results for  $C_L$  becomes more accurate. This accuracy is more visible at higher AOA.

### Investigating the effect of Reynolds number

We examined dependency of flow solution to the Reynolds number. Different Reynolds numbers are gained just by changing in scales of *Mesh3*. Figure 3 shows  $C_L$  for 3 different Reynolds number and compare them by no scale case ( $Re=8 \times 10^6$ ) and Thin Airfoil Theory. It is realized that by increasing the Reynolds number,  $C_L$  increases and becomes closer to Thin Airfoil Theory.

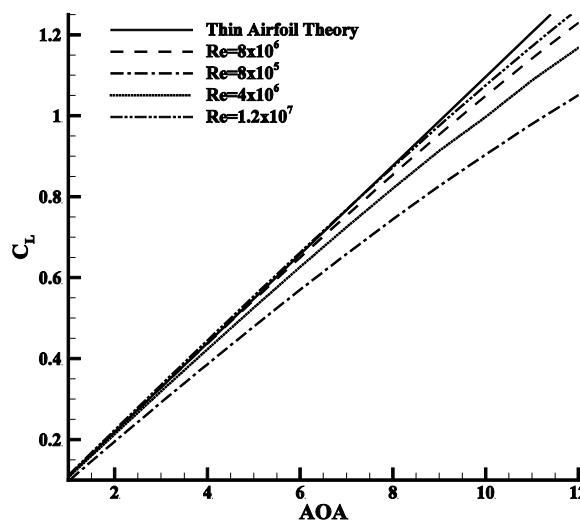


Fig.3  $C_L$  vs. angle of attack for different Reynolds Number compared with Thin Airfoil Theory [12]

### Pressure Coefficient

The mean static pressure on the surface, characterized by the pressure coefficient  $C_p$ , provides a more quantitative assessment of the accuracy of the numerical simulations. Figure 4-(a-c) compares the results of current simulation with numerical data at three angle of attacks (0, 10, 15 degree) provided by Ladson [1] and Gregory [14] using Spalart-Allmaras turbulence model. It is shown that there is a good agreement between the results of current simulation and numerical data reported in the literature [1, 14].

### Skin-Friction Coefficient

We had computed wall shear stress using *K- $\omega$  SST* turbulence model. Skin-friction coefficient has been plotted for upper surface of the airfoil at three AOA, as shown in Fig. 5. There is a good agreement between the current simulation and numerical results reported by Ladson [1]. For AOA=15, there is a slight difference between the current results and those of benchmark at  $X=0.1$ (m). This could be attributed to the requirement of creating finer mesh over the airfoil or improving turbulence model of the simulation.

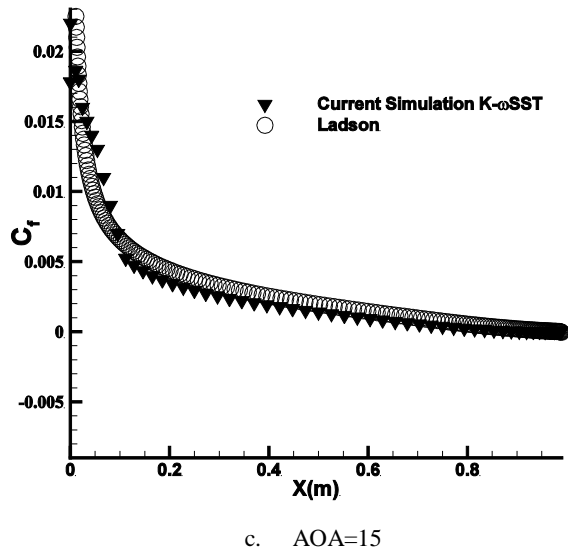
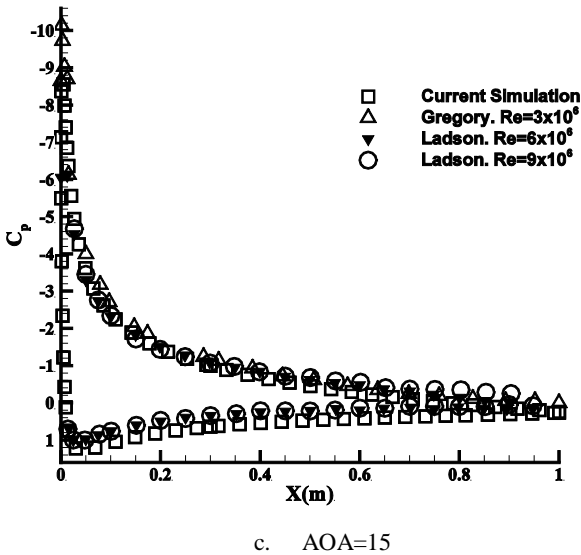
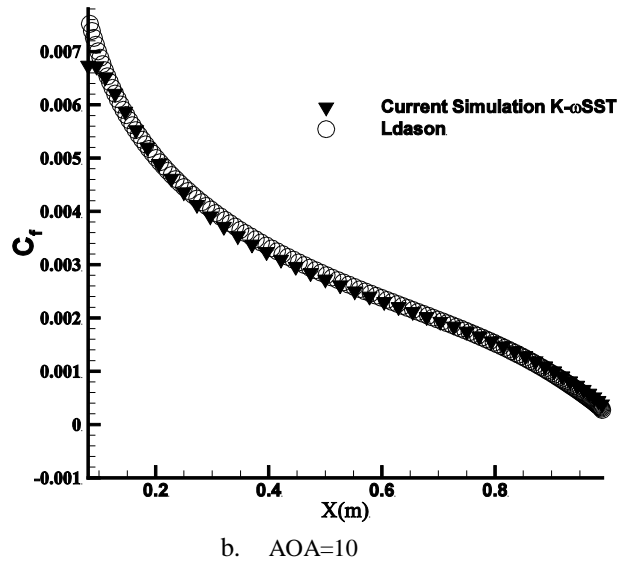
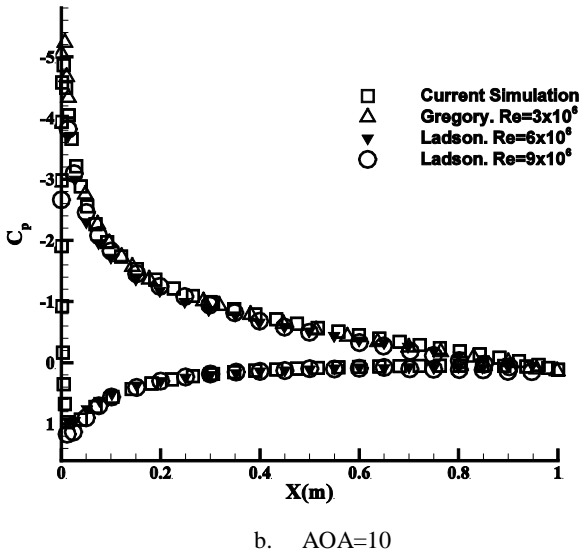
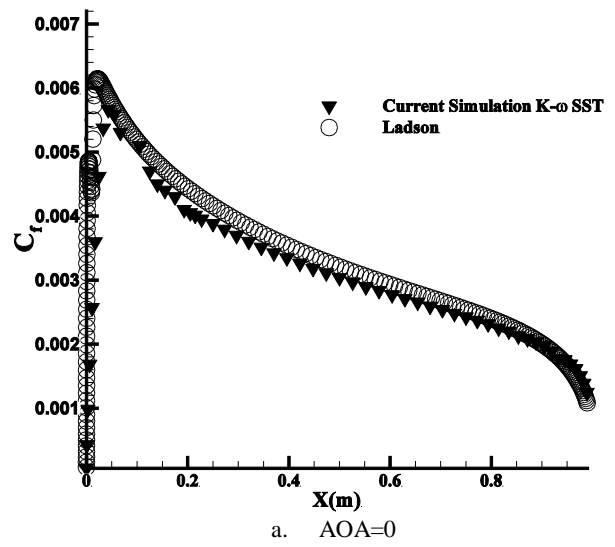
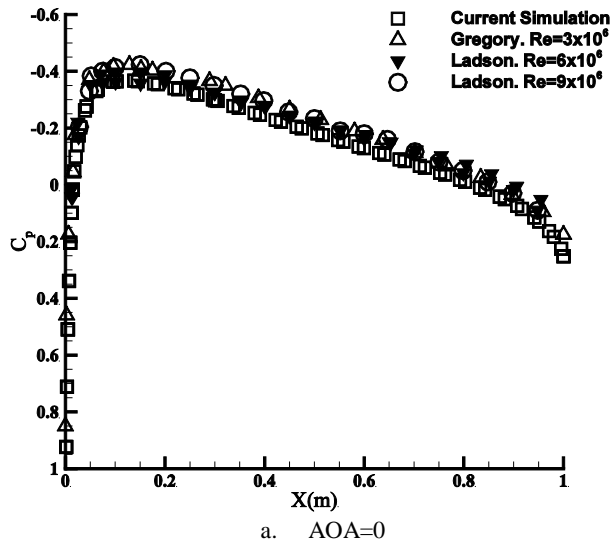


Fig. 4 Wall pressure Coefficient in  $Re=8 \times 10^6$  compared with Gregory [14] and Ladson [1]

Fig. 5 Wall skin-friction Coefficient at  $Re=8 \times 10^6$  using  $K-\omega$ SST turbulence model, compared with results of Ladson [1]

### Drag Coefficient

Drag coefficient from the current simulations has been computed using Spalart-Allmaras and  $K-\omega$ SST

turbulence models and compared with the experimental data of Abbot & von Doenhoff [12] and numerical data reported by Ladson [1]. The drag coefficient vs. lift coefficient is plotted in Fig. 6. It is shown that K- $\omega$ SST provided more accurate solution for drag coefficient compared to the Spalart-Allmaras solution. However, the accuracy of OpenFOAM simulation decreases as soon as AOA increases.

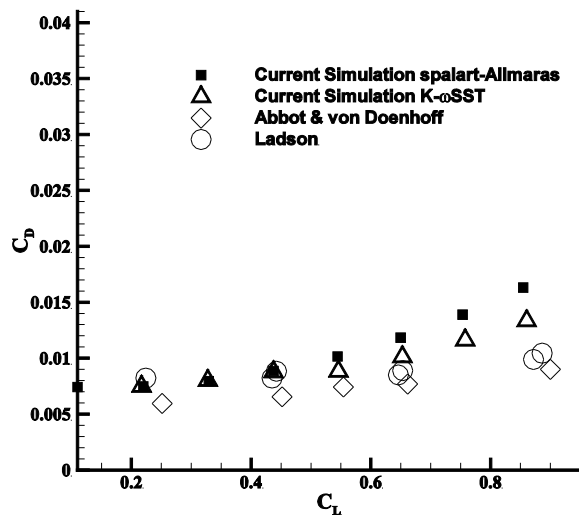


Fig. 6 Drag Coefficient at  $Re=8 \times 10^6$  from the current simulation (K- $\omega$ SST and Spalart-Allmaras turbulence models) compared with Ladson data [1].

## Conclusions

The main goal of the current work is investigation of the accuracy of OpenFOAM package for incompressible flow simulations over NACA0012 airfoil. We considered effect of mesh sizes, numerical discretization scheme, Reynolds number and turbulence modeling on the accuracy of solution. The best mesh is selected according to its accuracy for lift coefficient compared to Thin Airfoil Theory. Our examination of different discretization schemes of solution showed that use of fourth order scheme for pressure gradient and *linear* scheme for convective term of momentum equation provides the most accurate prediction for  $C_L$ . Via changing the Reynolds number of the flow over the airfoil, the accuracy of results have changed even for lift coefficient at high AOA. Our examinations showed that by increasing the Reynolds number, the results become closer to Thin Airfoil Theory. We assessed two different turbulence models and observed that K- $\omega$ SST model provides more accurate results for  $C_L$  and  $C_D$  compared to the Spalart-Allmaras one.

## References

- [1]-Ladson, C.H, "effects of Independent Variation of Mach and Reynolds Numbers on the Low-Speed Aerodynamics Characteristics of the NACA0012 Airfoil Section" NASA TM 4074 report, 1988.
- [2]-Moreau, S., Christophe, J. and Roger, M., "Les of the trailing-edge flow and noise of a NACA0012 airfoil near stall", Proceeding of the summer program, Center for Turbulence Research, 2008.

- [3]-IM, H.S. and Zha, G.C., "Delayed Detached Eddy Simulation of a Stall Flow over NACA0012 Airfoil Using High Order Schemes" AIAA 2011-1297.
- [4]-Verhoeven, O., "Trailing Edge Noise Simulations using IDDES in OpenFOAM", Master of Science Thesis, Delft University of Technology, 2011.
- [5]-Abedi, H., SimpleFoam tutorials, Chalmers University of Technology, November 2011.
- [6]-Tabor, H.G., Jask, H., Furbey, C., A tensorial approach to computational continuum mechanics using object-oriented techniques, *Comput. Phys.* (6) (1998).
- [7]-<http://www.openfoam.com>.
- [8]-OpenFOAM, OpenFoam user guide. 2011.
- [9]-Patankar, S.V., Numerical heat transfer and fluid flow, 1980: Hemisphere Pub. Corp.
- [10]-Spalart, P.R. and Allmaras, S. R., "A One-Equation Turbulence Model for aerodynamic flows," No. 1, 1994, pp.5-21.
- [11]-Menter, F.R., "Two-equation eddy-viscosity turbulence models for engineering applications", AIAA journal, 32(8), PP. 1598-1605, 1994.
- [12]-Abbott, Ira H. ; Von Doenhoff, Albert E., Theory of Wing Sections: Including a Summary of Airfoil Data (Dover Books on Aeronautical Engineering), 1945.
- [13]- "Turbulence Modeling Resources", NASA, Langley Research Center, October 2011.
- [14]-Gregory, N., O'Reilly, "Low-Speed Aerodynamics Characteristics of NACA0012 Airfoil Section, including the Effects of Upper-Surface roughness Simulating Hoar Frost" R. & M. No. 3726, 1973.